

Structure and Coulomb dissociation of ^{23}O within the quark-meson coupling model

R. Chatterjee^a, R. Shyam^b, K. Tsushima^{c,d}, A. W. Thomas^e

^aPhysics Department, Indian Institute of Technology, Roorkee, India

^bSaha Institute of Nuclear Physics, 1/AF Bidhan Nagar, Kolkata, India

^cSpecial Research Centre for the Subatomic Structure of Matter (CSSM), School of Chemistry and Physics, University of Adelaide, SA 5005, Australia

^dInternational Institute of Physics, Federal University of Rio Grande do Norte, Natal, Brazil

^eSpecial Research Centre for the Subatomic Structure of Matter (CSSM) and ARC Centre of Excellence in Particle Physics at Terascale (CoEPP), School of Chemistry and Physics, The University of Adelaide, SA 5005, Australia

Abstract

We study the ground-state structure of nuclei in the vicinity of the one-neutron dripline within the latest version of the quark-meson coupling (QMC) model with a particular emphasis on ^{23}O . For this nucleus the model predicts a $^{22}\text{O}(0^+) \otimes n2s_{1/2}$ configuration for its ground state, with a one neutron separation energy in close agreement with the corresponding experimental value. The wave function describing the valence neutron-core relative motion was then used to calculate the Coulomb dissociation of ^{23}O on a lead target at a beam energy of 422 MeV/nucleon. The experimental neutron-core relative energy spectrum and the total one-neutron removal cross sections are well described by the calculations. The widths of the longitudinal momentum distributions of the ^{22}O fragment are found to be broad, which do not support the formation of a neutron halo in this nucleus.

Keywords: Ground state structure of neutron dripline nuclei, quark-meson coupling model, structure and Coulomb dissociation of ^{23}O

PACS: 25.60.Gc, 12.39.Ki, 24.85.+p

1. Introduction

In recent years a lot of effort has been devoted to study the structure of the light neutron rich nuclei that have some unusual properties. For example, the neutron drip-line for the oxygen isotopes is located at ^{24}O (see e.g. Refs. [1]), and not at ^{28}O , the doubly magic nucleus that has been found to be unbound. This suggests that a new magic number appears at $N = 16$ in neutron rich nuclei. The reason for this observation has been investigated in several studies [2, 3]. Otsuka et al. [2] have suggested that it should be attributed to the spin-isospin dependent part of the nucleon-nucleon force yielding a strongly attractive interaction between a proton in $1d_{5/2}$ orbit and a neutron in $1d_{3/2}$ orbit, which in turn increases the gap between $2s_{1/2}$ and $1d_{3/2}$ orbitals for the $N=16$ oxygen isotope.

As the neutron drip-line is approached the nuclei experience weakening of the neutron binding energies, which leads to some special effects. The sudden rise of the interaction cross sections found in Refs. [4] for several lighter isotopes closer to the neutron drip-line was attributed to the extended density distribution(s) of the valence neutron(s) usually referred to as a neutron halo [5]. For oxygen isotopes a sudden rise of about 12% was observed [6] in the interaction cross sections between ^{22}O and ^{23}O . This led these authors to suggest ^{23}O as a candidate for a neutron-halo system. However, there are several other observations that are not consistent with this picture. The valence neutron in ^{23}O is relatively strongly bound, with a one neutron separation energy (S_{-n}) of 2.74 MeV, which is in contrast to the well established one neutron halo nuclei like, ^{11}Be and ^{19}C , that have S_{-n} of only about 0.5 MeV. Thus the last neutron in ^{23}O should not extend to larger distances. Furthermore, the longitudinal momentum ($p_{||}$) (with respect to the reaction plane) distributions (LMD) of the ^{22}O fragment have been measured [7, 8, 9, 10] in the breakup reactions of ^{23}O on lighter target nuclei, where the widths of these distributions are found to be in excess of 100 MeV/c. This is about 2-3 times larger than those observed in the cases of ^{11}Be and ^{19}C induced reactions (see, e.g. Ref. [11]). A narrow LMD is a direct signature of the development of the halo structure (see, e.g. the discussions presented in [12]).

Moreover, there has been a disagreement in the assignment of the ground state spin-parity (J^π) of ^{23}O nucleus among various authors. In Ref. [7], from the LMD measurements of the ^{22}O and ^{21}O fragments in the ^{23}O induced reaction on a carbon target, it was concluded that the data support a J^π of $\frac{5}{2}^+$. However, this conclusion was not supported by the measurements of the ^{23}O breakup reactions reported in Ref. [9, 13] where a J^π of $\frac{1}{2}^+$ was found to be consistent with the data. In Ref. [14] the interaction cross sections of ^{22}O and ^{23}O isotopes were measured on a carbon target and it was concluded that these data are more in agreement with a $^{22}\text{O} + \text{valence neutron}$ in the $2s_{1/2}$ picture of the ^{23}O nucleus. This would imply a J^π of $\frac{1}{2}^+$. These conflicting experimental results call for a more rigorous theoretical investigation of the ^{23}O ground state configuration. Furthermore, there is a need to analyze the data on the breakup reactions of ^{23}O within a more microscopic theoretical model than has been employed so far.

The aim of this paper is to investigate within the quark-meson coupling (QMC) model, the ground state structure of several light neutron rich nuclei that lie in the vicinity of the one-neutron dripline with a particular attention to the ^{23}O nucleus. The QMC model is a quark-based model for nuclear matter, finite nuclei and hypernuclei [15, 16, 17, 18, 19, 20], where quarks in the non-overlapping MIT bags interact self consistently with isoscalar-scalar (σ) and isoscalar-vector (ω) mesons in the mean field approximation. The explicit treatment of the nucleon internal structure is a key point of this model and it represents an important departure from quantum hadrodynamics (QHD) [21]. The self-consistent response of the bound light quarks to the mean σ field leads to a new saturation mechanism for nuclear matter [15].

Although formulated as a relativistic mean field theory with just a few parameters (determined from the properties of nuclear matter), QMC model has been shown to lead to a remarkably realistic Skyrme force [22, 23]. This has led to its application to describe rather successfully several properties (e.g. binding energies per particle, density and charge distributions and energy levels) of closed shell nuclei [19, 23] with masses

spanning a wide range of the periodic table. The agreement with the corresponding experimental data is not been inferior to that obtained within the Skyrme Hartree-Fock (HF) or relativistic mean field (RMF) models.

The same effective interaction (with identical parameters) has also been used to describe the properties of nuclei far from stability in Ref. [23] where this model was used to predict the positions of the two-neutron drip line in Ni and Zr isotopes. In this study the pairing correlation between two neutrons has been treated in a Hartree-Fock-Bogoliubov (HFB) approach. In these calculations the neutron drip line appears around the neutron numbers that are similar to the predictions provided by the Skyrme force SLy4 commonly used in the non-relativistic calculations [24]. Furthermore, the shell quenching, which has important consequences for the astrophysical rapid capture process, is also very close to that obtained in the Skyrme-Hartree-Fock-Bogoliubov approach in Ref. [24]. It is remarkable because, unlike the non-relativistic Skyrme force based calculations where the experimental values for the binding energy and the radii are included in the fitting procedure for determining the corresponding parameters, in the QMC calculations the parameters remain the same and these quantities are actually predicted by the model. Therefore, the QMC model contains features that make it appealing to apply to the description of the structure of the drip line nuclei.

In this paper we report the results of the QMC model calculations for the light neutron rich nuclei that lie in the vicinity of one-neutron dripline - a region which has not been explored within this model so far. We use the latest version of the QMC model (to be referred to as QMC-III) [20] to predict the one-neutron separation energy and the valence neutron spin-parity in the ground state of the neutron rich nuclei ^{23}N , ^{23}O , ^{31}Ne , ^{35}Mg , ^{37}Na , ^{45}S . Our particular attention will be focused on the ^{23}O nucleus where we use this model to calculate also the neutron and proton density distributions in order to investigate the possible existence of a halo structure in this nucleus. Furthermore, we use the predicted valence neutron configuration in the ground state of ^{23}O and the corresponding valence neutron-core wave function to investigate its Coulomb dissociation (CD) on a Pb target, for which some data exists [13] on the valence neutron-core relative energy differential and the total one-neutron removal cross sections.

In the next section, our formalism is presented where some important features of the QMC model are discussed. In this section we also presented a short review of the CD model that has been used to calculate the valence neutron-core relative energy differential and the total one-neutron removal cross sections for the breakup of ^{23}O on a Pb target. Our results are presented and discussed in section 3. A summary and conclusions of our work is presented in section 4.

2. Formalism

2.1. Quark-meson coupling model

The QMC-III model includes the self-consistent effect of the mean scalar field on the familiar one-gluon exchange hyperfine interaction [25] that in free space leads to the $N - \Delta$ and $\Sigma - \Lambda$ mass splitting. With this development, QMC model has been able to explain the properties of Λ hypernuclei for the s -state rather well, although the p - and d -states tend to be underbound. It also maintains the very natural explanation

of the small spin-orbit force in the Λ -nucleus interaction that was found in an earlier version of the QMC model (to be referred to as QMC-I) [17, 18, 26]. In QMC-III, while the quality of results for Λ and Ξ hypernuclei is comparable to that obtained in QMC-I [18], no bound states for the Σ states [20] were found in medium and heavy mass nuclei. This finding, which is a consequence of the extra repulsion associated with the increased one-gluon-exchange hyperfine interaction in medium, is in agreement with the non-observation of such states experimentally. The QMC-III model has recently been used [27] to study the production of Ξ^- hypernuclei via the (K^-, K^+) reaction, which is currently of great interest at the J-PARC facility in Japan.

In order to calculate the properties of the finite nuclei, we construct a simple, relativistic shell model with self-consistent scalar and vector mean fields. The Lagrangian density for a nuclear system in the QMC model is written as [17]:

$$\begin{aligned} \mathcal{L}_{QMC} = & \bar{\psi}_N(\mathbf{r})[i\boldsymbol{\gamma} \cdot \boldsymbol{\partial} - M_N(\sigma) - (g_\omega\omega(\mathbf{r}) + g_\rho\frac{\boldsymbol{\tau}_3^N}{2}b(\mathbf{r}) + \frac{e}{2}(1 + \boldsymbol{\tau}_3^N)A(\mathbf{r}))\boldsymbol{\gamma}_0]\psi_N(\mathbf{r}) \\ & - \frac{1}{2}[(\nabla\sigma(\mathbf{r}))^2 + m_\sigma^2\sigma(\mathbf{r})^2] + \frac{1}{2}[(\nabla\omega(\mathbf{r}))^2 + m_\omega^2\omega(\mathbf{r})^2] \\ & + \frac{1}{2}[(\nabla b(\mathbf{r}))^2 + m_\rho^2b(\mathbf{r})^2] + \frac{1}{2}(\nabla A(\mathbf{r}))^2. \end{aligned} \quad (1)$$

Here $\psi_N(\mathbf{r})$, $b(\mathbf{r})$, $\omega(\mathbf{r})$ and $A(\mathbf{r})$ are, respectively, the nucleon, the ρ meson, the ω meson and Coulomb fields, while m_σ , m_ω and m_ρ are the masses of the σ , ω and ρ mesons. g_ω and g_ρ are the ω -N and ρ -N coupling constants that are related to the corresponding (u,d)-quark- ω , g_ω^q , and (u, d)-quark- ρ , g_ρ^q , coupling constants as $g_\omega = 3g_\omega^q$ and $g_\rho = g_\rho^q$, and e is the proton charge.

The following equations of motion are obtained from the Lagrangian density Eqs. (1):

$$[i\boldsymbol{\gamma} \cdot \boldsymbol{\partial} - M_N(\sigma) - (g_\omega\omega(\mathbf{r}) + g_\rho\frac{\boldsymbol{\tau}_3^N}{2}b(\mathbf{r}) + \frac{e}{2}(1 + \boldsymbol{\tau}_3^N)A(\mathbf{r}))\boldsymbol{\gamma}_0]\psi_N(\mathbf{r}) = 0, \quad (2)$$

$$(-\nabla_r^2 + m_\sigma^2)\sigma(\mathbf{r}) = g_\sigma C_N(\sigma)\rho_s(\mathbf{r}), \quad (3)$$

$$(-\nabla_r^2 + m_\rho^2)b(\mathbf{r}) = \frac{g_\rho}{2}\rho_3(\mathbf{r}), \quad (4)$$

$$(-\nabla_r^2)A(\mathbf{r}) = e\rho_p(\mathbf{r}), \quad (5)$$

where, $\rho_s(\mathbf{r})$, $\rho_B(\mathbf{r}) = \rho_p(\mathbf{r}) + \rho_n(\mathbf{r})$, $\rho_3(\mathbf{r}) = \rho_p(\mathbf{r}) - \rho_n(\mathbf{r})$ and $\rho_p(\mathbf{r})$ ($\rho_n(\mathbf{r})$) are the scalar, baryon, third component of isovector, and proton (neutron) densities [18]. On the right hand side of Eq. (3), a new and characteristic feature of QMC appears, arising from the internal structure of the nucleon, namely, $g_\sigma C_N(\sigma) = -\frac{\partial M_N(\sigma)}{\partial \sigma}$, where $g_\sigma \equiv g_\sigma(\sigma = 0)$. We use the density dependent nucleon mass $M_N(\sigma)$ as parameterized in Ref. [20].

The coupled non-linear differential Eqs. (2)-(5) can be solved by a standard iteration procedure as discussed in, e.g., Refs. [28]. The coupling constants g_σ , g_ω , g_ρ , and masses m_σ , m_ω and m_ρ have been taken to be the same as those given in Ref. [20]. To calculate the nuclear levels we use a relativistic shell model (see, eg. Refs. [17, 19] for more details).

2.2. The Coulomb dissociation model

The model used to calculate the CD cross sections of the ^{23}O nucleus is described in detailed in Refs. [29, 30, 31]. Therefore, we give here only a brief sketch of it. This theory is formulated within the post-form finite range distorted wave Born approximation (FRDWBA), where the electromagnetic interaction between the fragments and the target nucleus is included to all orders and the breakup contributions from the entire nonresonant continuum corresponding to all the multipoles and the relative orbital angular momenta between the fragments are taken into account [30]. Only the full ground state wave function of the projectile, of any orbital angular momentum configuration, enters in this theory as input. Thus, unlike most of the theoretical models described in a recent review of breakup theories [32], this approach does not require the knowledge of the positions and widths of the continuum states. Hence, it is free from the uncertainties associated with the multipole strength distributions [33] that may exist in some of these theories.

We consider a breakup reaction ($a+A \rightarrow b+c+A$), where the projectile a breaks up into fragments b (charged) and c (uncharged) in the Coulomb field of a target A . The differential cross section for the relative energy distribution for this reaction is given by

$$\frac{d\sigma}{dE_{bc}} = \int_{\Omega_{bc}, \Omega_{aA}} d\Omega_{bc} d\Omega_{aA} \left\{ \sum_{lm} \frac{1}{(2l+1)} |\beta_{lm}|^2 \right\} \frac{2\pi}{\hbar v_{aA}} \frac{\mu_{bc} \mu_{aA} p_{bc} p_{aA}}{h^6}, \quad (6)$$

where v_{aA} is the a - A relative velocity in the entrance channel, Ω_{bc} and Ω_{aA} are solid angles, μ_{bc} and μ_{aA} are reduced masses, and p_{bc} and p_{aA} are appropriate linear momenta corresponding to the b - c and a - A systems, respectively.

The reduced amplitude, β_{lm} , in the post-form FRDWBA is given by

$$\beta_{lm} = \langle \exp(\gamma \mathbf{k}_c - \alpha \mathbf{K}) | V_{bc} | \Phi_a^{lm} \rangle \langle \chi_b^{(-)}(\mathbf{k}_b) \chi_c^{(-)}(\delta \mathbf{k}_c) | \chi_a^{(+)}(\mathbf{k}_a) \rangle, \quad (7)$$

where \mathbf{k}_b , \mathbf{k}_c are Jacobi wave vectors of fragments b and c , respectively, in the final channel of the reaction, \mathbf{k}_a is the wave vector of projectile a in the initial channel and V_{bc} is the interaction between b and c . Φ_a^{lm} is the ground state wave function of the projectile with relative orbital angular momentum state l and projection m . In the above, \mathbf{K} is an effective local momentum associated with the core-target relative system, whose direction has been taken to be the same as the direction of the asymptotic momentum \mathbf{k}_b [29]. α , δ , and γ in Eq. (5), are mass factors relevant to the Jacobi coordinates of the three body system (see Fig. 1 of Ref. [29]). The wave functions $\chi_b^{(-)}$ and $\chi_c^{(-)}$, are the distorted waves for the relative motion of b and c with respect to A and the c.m. of the b - A system, respectively, with ingoing wave boundary condition and $\chi_a^{(+)}(\mathbf{k}_a)$ is the distorted wave for the scattering of the c.m. of the projectile a with respect to the target with outgoing boundary conditions.

The first term in Eq. (7) contains the structure information about the projectile through the ground state wave function Φ_a^{lm} , while the second term is associated with the dynamics of the reaction. For the pure Coulomb case, $\chi_b^{(-)}(\mathbf{k}_b)$ and $\chi_a^{(+)}(\mathbf{k}_a)$ are replaced by the appropriate Coulomb distorted waves, and $\chi_c^{(-)}(\delta \mathbf{k}_c)$ by a plane wave as the fragment c is uncharged (e.g. for a neutron). This allows the second term of Eq. (7) to be evaluated analytically in terms of the bremsstrahlung integral [34]. A

Table 1: Valence neutron separation energy as calculated in the QMC model. The second column shows the quantum number of the valence neutron in each case.

Isotope	valence neutron orbit	S_{-n}^{QMC} (MeV)	S_{-n}^{data} (MeV)
^{23}N	$^2s_{1/2}$	-2.701	-2.494 ± 0.360
^{23}O	$^2s_{1/2}$	-2.858	-2.740 ± 0.130
^{31}Ne	$^1f_{7/2}$	-0.004	-0.290 ± 1.640
^{35}Mg	$^1f_{7/2}$	-0.861	-0.728 ± 0.463
^{37}Na	$^1f_{7/2}$	-1.054	-0.750 ± 0.180
^{45}S	$^2p_{3/2}$	-1.592	-2.208 ± 1.786
^{49}Ar	$^2p_{3/2}$	-2.726	-2.501 ± 0.590

more detailed description of the evaluation of the reduced amplitude β_{lm} can be found in Refs. [29, 35]. It is clear from Eqs. (6) and (7) that within this model of breakup reactions, explicit information about the continuum strength distribution of the projectile is not required in calculations of the relative energy spectra - the entire continuum is automatically included in this theory.

It should be remarked that this model of the Coulomb dissociation belongs to one particular class of breakup theories that include the interaction between the projectile fragments and the target nucleus to all orders but treat the fragment-fragment interaction in first order. Because for relative energies of our interest there are no resonances in the $n+^{22}\text{O}$ continuum, we expect this approximation to be valid. It is clearly a good approximation for the deuteron and the neutron halo systems [33]. For those cases where higher order effects of the fragment-fragment interaction are known to be nonnegligible, this model will have a limited applicability. Recently, calculations are becoming available where the breakup reactions are treated in terms of the Faddeev type of theories of the three-body problem including also the Coulomb potentials in the fragment-target and fragment-fragment interactions [36, 37, 38]. These studies although confined so far mostly to breakup reactions on a proton target, are expected to provide a comprehensive check on various approximations used in different types of breakup theories [39].

3. Results and discussions

In Table 1, we show the one-neutron separation energies (S_{-n}) and the valence neutron quantum numbers of a number of light neutron rich nuclei lying in the vicinity of the one-neutron dripline. In the last column of this table we show the experimental value of S_{-n} (S_{-n}^{data}) that have been derived from Refs. [40, 41, 42, 43]. It is clear that S_{-n} predicted by the QMC model is in reasonable agreement with the corresponding experimental value for all the nuclei studied in table 1. This is remarkable in view of the fact that in these calculations the model parameters were the same as those used in the description of the normal nuclei in Ref. [20]. It may however, be remarked that for still

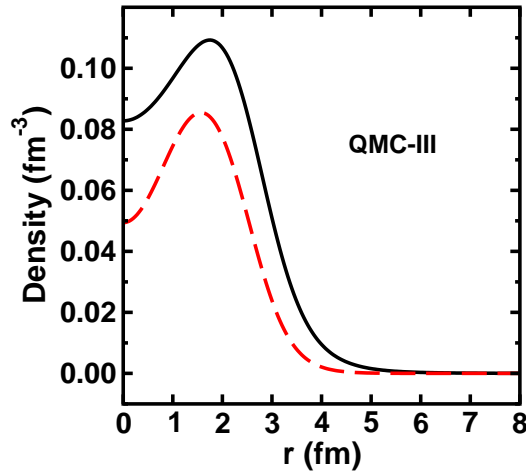


Figure 1: (Color online) Neutron (solid line) and proton (dashed line) density distributions for ^{23}O in QMC-III model.

lighter nuclei (e.g. isotopes of C and Be etc.) the QMC model may not be applicable as the mean field approximation is unlikely to be valid for these systems. For example, we found that for ^{19}C the QMC model predicts a S_{-n} of -1.192 MeV (-3.095 MeV) for a ground configuration in which a $2s_{1/2}$ ($1d_{5/2}$) neutron is bound to a 0^+ ^{18}O core. However, a generally accepted value of S_{-n}^{data} for this nucleus is 0.576 ± 0.094 MeV with a ground state spin-parity of $\frac{1}{2}^+$ [44, 45, 46], even though there is still some uncertainty in the mass of ^{19}C . It has been shown earlier [47, 48] that the valence neutron in ^{19}C is no longer attached to a mean field orbital. Thus, the mean-field dynamics has ceased to be the dominant source of binding in this case where the dynamical valence neutron-core interaction provides most of the binding. Therefore, a deviation of the S_{-n} calculated in the QMC model for this nucleus from the corresponding experimental value is not surprising. Nevertheless, it is interesting to note that the ground state configuration $^{18}\text{C}(0^+) \otimes n2s_{1/2}$ leads to a S_{-n} more in agreement with its experimental value, which is in line with the conclusions of Refs. [44, 45, 46].

As we are particularly interested in the nucleus ^{23}O , we discuss our results in some details for this case. In table 1 we notice that, the configuration where valence neutron lies in the $2s_{1/2}$ level (with ^{22}O remaining as inert core), yields a S_{-n} value of 2.86 MeV. This is very close to the experimental value of 2.74 MeV for this quantity. We have also tried a scheme to get a valence neutron spin-parity of $\frac{5}{2}^+$ by filling the last neutron orbit ($2s_{1/2}$) with two neutrons. This, however, makes the ^{23}O isotope unstable in our model. Therefore, we confirm that the ground state of this nucleus is consistent with a $^{22}\text{O}(0^+) \otimes 2s_{1/2}$ configuration with a one neutron separation energy of 2.86 MeV. It should be mentioned here that using the QMC-I model, we find a one neutron binding energy of 4.34 MeV within the same ground state configuration. Thus, the extra effects put into the QMC-III model (e.g., one-gluon exchange hyperfine interaction) do seem to be important to describe self-consistently the structure of the drip-line nuclei.

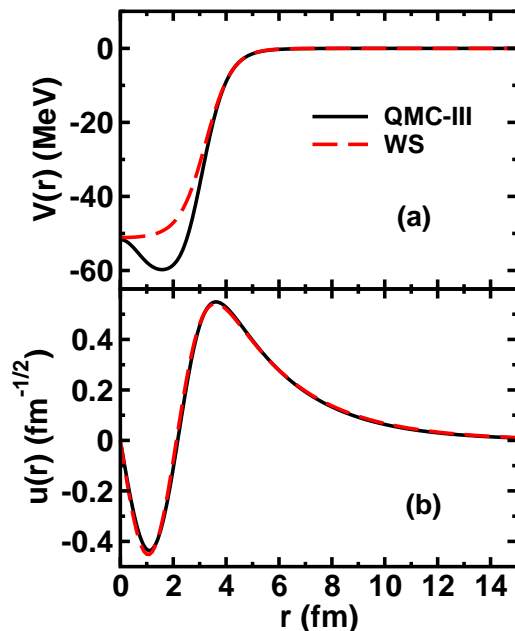


Figure 2: (Color online) The QMC-III (solid line) and Woods-Saxon (dashed line) valence neutron-core potentials [part (a)] and corresponding wave functions [part (b)] for the ^{23}O nucleus.

In Fig. 1, we show the neutron and proton density distributions for ^{23}O obtained within the QMC-III model. We see that the central density of the neutron distribution is clearly larger than that of the proton. At the same time the surface diffuseness of the two distributions are almost identical. This is consistent with the criteria for a neutron skin [49, 3]. The neutron skin thickness, which is the difference between the neutron and proton root mean square radii (RMS) [50] is found to be 0.46 fm, which is in agreement with the value reported for this nucleus in Ref. [3] where calculations have been performed within a QHD type of relativistic mean field model. In neutron rich isotopes of several medium to heavy mass nuclei, a neutron skin of similar thickness has been reported by several authors (see, e.g. Refs. [51]).

In Figs. 2a and 2b, we show the valence neutron-core potential and the corresponding wave function, respectively, for the ^{23}O nucleus calculated within the QMC-III model. The potential is the sum of scalar and vector fields and the wave function is only the upper component of the spinor, as the corresponding lower component is at least two orders of magnitude smaller. For comparison, we also show a Woods-Saxon (WS) potential and the respective wave function for this system. This potential has been parameterized by adjusting its depth to reproduce the experimental value of S_n with the radius and diffuseness parameters of 1.15 fm and 0.5 fm, respectively. We note that while the QMC-III potential is somewhat deeper than the WS potential at smaller distances, they are similar in the surface region. However, the wave functions generated by the two potentials are almost identical at all radii.

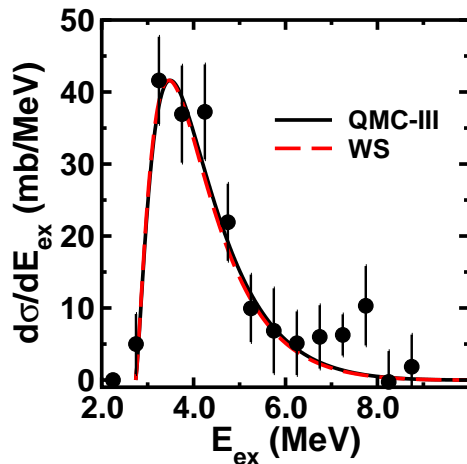


Figure 3: (Color online) The calculated excitation energy spectra in the Coulomb dissociation of ^{23}O on a Pb target at 422 MeV/nucleon beam energy obtained with QMC-III (solid line) and Woods-Saxon (dashed line) wave function. The data is taken from Ref. [13]. The calculated cross sections are normalized to the peak of the experimental data in each case.

The wave functions calculated above have been used to investigate the Coulomb dissociation (CD) of the ^{23}O nucleus on Pb target, for which some data exists [13] on the valence neutron-core relative energy differential cross section and the total one-neutron removal cross sections. The CD process has a number of advantages. It is free from the uncertainties associated with the nuclear interactions. Moreover the inelastic breakup mode (also known as stripping or breakup fusion) is absent in the pure Coulomb dissociation reactions. Therefore, this process is ideally suited for probing the structure of the projectile.

In Fig. 3, the calculated energy differential cross section ($\frac{d\sigma}{dE_x}$) is shown as a function of the excitation energy ($E_x = E_{bc} + S_{-n}$, where E_{bc} is the n - ^{22}O relative energy). The results obtained with QMC-III (solid line) as well as a WS ground state (dashed line) wave functions are displayed. In getting these cross sections, an integration has been carried out over θ_{aA} up to the grazing angle of the reaction. In order to compare the calculations with the data of Ref. [13], the calculated cross sections need to be convoluted with the detector response function of the experiment. Since this is not available to us we have normalized our cross sections to the peak of the experimental $\frac{d\sigma}{dE_x}$ in each case. This may be viewed as an alternative to the convolution procedure.

We note that our calculations are able to describe the shape of the relative energy spectrum quite well over the entire region of excitation energies. The sharp rise of the experimental cross section just after the threshold is quite well reproduced. Even the widths of the experimental distribution is well reproduced in our model. In contrast to this, the width of the distribution is grossly over predicted within a semiclassical breakup model using plane waves for the relative motion wave functions in the outgoing channel, as shown in Ref. [13]. Once optical potentials are used to describe the n

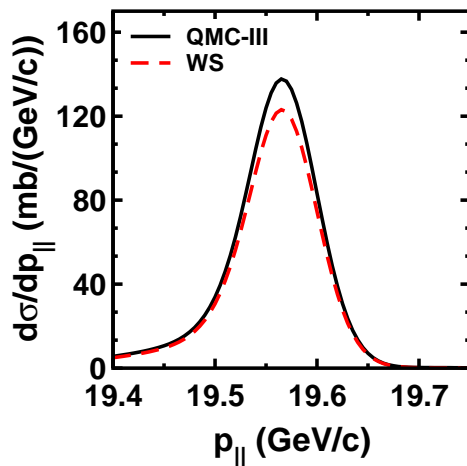


Figure 4: (Color online) The calculated longitudinal momentum distribution of ^{22}O fragment in the Coulomb dissociation of ^{23}O on a Pb target at 422 MeV/nucleon beam energy obtained with QMC-III (solid line) and Woods-Saxon (dotted line) wave function.

^{22}O relative motion, the situation improves. ,

The total electromagnetic one-neutron removal cross sections obtained in our CD model is 79.26 mb and 77.15 mb with QMC-III and WS wave functions, respectively. This is only about 10% smaller than the lower limit of the corresponding experimental value of 97 ± 10 mb [13]. However, since the upper limit of uncertainty in the experimental data is of the order of 20% [13], this slight under prediction of the total electromagnetic cross sections by our model is not significant.

In Fig. 4, we show the calculated LMD for the ^{22}O fragment emitted in the CD of ^{23}O on a Pb target at 422 MeV/c beam energy, calculated with QMC-III and WS ground state wave functions. The full width at half maximum (FWHM) of the LMD is about 85 MeV/c in both cases. This value is more than a factor 2 larger than the FWHM of the LMD of the core fragment observed in reactions induced by established one-neutron halo nuclei like ^{11}Be and ^{19}C . Although there are no data available for the LMD of the ^{22}O fragment in the ^{23}O induced reaction on a heavier target like Pb, the FWHM of the LMD of ^{22}O have been measured in the ^{23}O induced breakup reaction on light targets like carbon [7, 9, 10], where they have been found to lie around 100 MeV/c. Therefore, these results almost rule out the development of a one-neutron halo structure in ^{23}O , even though the valence neutron occupies an s-orbit in this nucleus.

4. Summary and conclusions

In summary, we have studied the ground state structure and the one neutron separation energies of a number of light mass neutron rich nuclei lying in the vicinity of one-neutron drip line within the latest version of the quark-meson coupling model. With the same set of parameters that were used to describe the properties of normal nu-

clei, we obtain a reasonable agreement with the experimental one-neutron separation energies. We concentrated particularly on the ^{23}O nucleus. Our calculations confirm a $^{22}\text{O}(0^+) \otimes 2s_{1/2}$ configuration for the ground state of this nucleus with a one neutron separation energy of 2.86 MeV that is in close agreement with the corresponding experimental value. A spin-parity assignment of $1d_{5/2}$ to this nucleus is not supported by our model. We predict the development of the neutron skin in this nucleus with a thickness of 0.48 fm.

The valence neutron-core wave function calculated within the QMC model has been used to study the Coulomb dissociation of ^{23}O on a Pb target at the beam energy of 422 MeV/c employing a theory that requires only the ground state projectile wave function as input and is free from any other adjustable parameter. Although at this beam energy the relativistic effects play a role [52], yet a fully quantal relativistic theory of breakup reactions is not yet available. Our theory is essentially non-relativistic in nature. Nevertheless, we observe that the existing data on the excitation energy spectra and the total electromagnetic one-neutron removal cross section are well reproduced. The calculated longitudinal momentum distributions of the ^{22}O fragment are broad, which effectively excludes the development of a one-neutron halo structure in this nucleus even though the valence neutron occupies an s -orbit. Our study shows that the latest quark-meson coupling model provides a competitive alternative for describing the structure of the drip line nuclei as compared to the commonly used non-relativistic models.

5. Acknowledgments

This work has been supported by the University of Adelaide and the Australian Research Council through grant FL0992247(AWT) and through the ARC Centre of Excellence for Particle Physics at the Terascale. KT was also supported by a visiting professorship of International Institute of Physics, Federal University of Rio Grande do Norte, Natal, Brazil.

References

- [1] D. Guillemaud-Mueller *et al.*, Phys. Rev. C **41** (1990) 937; H. Sakurai *et al.*, Phys. Lett. **B448** (1999) 180; A. Ozawa *et al.*, Nucl. Phys. **A673** (2000) 411; C. R. Hoffman *et al.*, Phys. Lett. **B672** (2009) 17.
- [2] T. Otsuka *et al.*, Phys. Rev. Lett. **87** (2001) 082502; M. Stanoiu *et al.*, Phys. Rev. C **69** (2004) 034312.
- [3] W. Z. Jiang, Y. L. Zhao, Z. Y. Zhu, and S. F. Shen, Phys. Rev. C **72** (2005) 024313.
- [4] I. Tanihata *et al.*, Phys. Rev. Lett. **55** (1985) 2676; I. Tanihata *et al.*, Phys. Lett. **B206** (1988) 592.
- [5] G. Hansen and B. Jonson, Europhys. Lett. **4** (1987) 409.
- [6] R. Kanungo, I. Tanihata and A. Ozawa, Phys. Lett. **B512** (2001) 261.

- [7] R. Kanungo *et al.*, Phys. Rev. Lett. **88** (2002) 142502.
- [8] E. Sauvan *et al.*, Phys. Rev. C **69** (2004) 044603.
- [9] D. Cortina-Gil *et al.*, Phys. Rev. Lett. **93** (2004) 062501.
- [10] C. Rodriguez-Tajes *et al.*, Phys. Rev. C **82** (2010) 024305.
- [11] B. Jonson, Phys. Rep. **389** (2004) 1, and references therein.
- [12] C. A. Bertulani, L. F. Canto and M S. Hussein, Phys. Rep. **226** (1993) 281.
- [13] C. Nociforo *et al.*, Phys. Lett. **B605** (2005) 79.
- [14] R. Kanungo *et al.*, Phys. Rev. C **84** (2011) 061304 (R).
- [15] P. A. M. Guichon, Phys. Lett. **B200**, 235 (1988).
- [16] P. A. M. Guichon, K. Saito, E. N. Rodionov and A. W. Thomas, Nucl. Phys. A **601** (1996) 349.
- [17] K. Saito, K. Tsushima, A. W. Thomas, Nucl. Phys. **A609** (1996) 339.
- [18] K. Tsushima, K. Saito, J. Haidenbauer and A. W. Thomas, Nucl. Phys. A **630** (1998) 691.
- [19] K. Saito, K. Tsushima, A. W. Thomas, Prog. Part. Nucl. Phys. **58** (2007) 1.
- [20] P. A. M. Guichon, A. W. Thomas and K. Tsushima, Nucl. Phys. A **814** (2008) 66; K. Tsushima and P. A. M. Guichon, AIP Conf. Proc. **1261** (2010) 232.
- [21] B. D. Serot and J. D. Walecka, Adv. Nucl. Phys. **16** (1986) 1; *ibid.*, Int. J. Mod. Phys. E **6** (1997) 515.
- [22] P. A. M. Guichon and A. W. Thomas, Phys. Rev. Lett. **93** (2004) 132502.
- [23] P. A. M. Guichon, H. H. Matevosyan, N. Sandulescu and A. W. Thomas, Nucl. Phys. A **772** (2006) 1.
- [24] E. Chanabat, P. Bonche, P. Haensel, J. Meyer, and R. Schaeffer, Nucl. Phys. A **635** (1998) 231.
- [25] J. Rikovska-Stone, P. A. M. Guichon, H. H. Matevosyan and A. W. Thomas, Nucl. Phys. **A792** (2007) 341.
- [26] K. Tsushima, K. Saito and A. W. Thomas, Phys. Lett. B **411** (1997) 9; [Erratum-*ibid.* B **421** (1998) 413].
- [27] R. Shyam, K. Tsushima and A. W. Thomas, Nucl. Phys. A **881** (2012) 255.
- [28] C. J. Horowitz and B. D. Serot, Nucl. Phys. **A368** (1981) 503; C. J. Horowitz, D. P. Murdoch and B. D. Serot, Computational Nuclear Physics, Vol. 1, Ed. K. Langanke, J. A. Maruhn and S. E. Koonin (Springer, Berlin, 1991), p. 129.

- [29] R. Chatterjee, P. Banerjee and R. Shyam, Nucl. Phys. **A675** (2000) 477.
- [30] P. Banerjee, G. Baur, K. Hencken, R. Shyam, and D. Trautmann, Phys. Rev. C **65** (2002) 064602
- [31] P. Banerjee, R. Chatterjee and R. Shyam, Phys. Rev. C **78** (2008) 035804.
- [32] D. Baye and P. Capel, Lecture Notes in Physics **848**, p. 121 (Springer, Berlin, 2012).
- [33] G. Baur, K. Hencken and D. Trautmann, Prog. Part. Nucl. Phys. **51** (2003). 487.
- [34] A. Nordsieck, Phys. Rev. **93** (1954) 785.
- [35] R. Shyam and P. Danielewicz, Phys. Rev. C **63** (2001) 054608.
- [36] A. Deltuva and A. C. Fonseca, Phys. Rev. C **79** (2009) 014606.
- [37] R. Crespo, A. Deltuva, M. Rodriguez-Gallardo, E. Cravo and A.C. Fonseca, Phys. Rev. C **79** (2009) 014609.
- [38] E. Cravo, R. Crespo, A. M. Moro, A. Deltuva, Phys. Rev. C **81** (2010) 031601.
- [39] N. J. Upadhyay, A. Deltuva and F. M. Nunes, Phys. Rev. C **85** (2012) 054621.
- [40] L. Gaudefroy et al., Phys. Rev. Lett. **109** (2012) 202503.
- [41] B. Jurado *et al.*, Phys. Lett. B **649** (2007) 43.
- [42] G. Audi, A. H. Wapstra, and C. Thibault, Nucl. Phys. A **729** (2003) 337.
- [43] P. M. Endt, Nucl. Phys. **A633** (1998) 1.
- [44] T. Nakamura *et al.*, Phys. Rev. Lett. **83** (1999) 1112.
- [45] P. Banerjee and R. Shyam, Phys. Rev. C **61** (1999) 047301.
- [46] P. Descouvemont, Nucl. Phys. A **675** (2000) 559.
- [47] H. Lenske, C. M. Keil and F. Hofmann, Prog. Part. Nucl. Phys. **46** (2001) 187.
- [48] H. Lenske, C. M. Keil and F. Hofmann, Proc. Int. Conf. Nuclear Physics at the Border Lines, World Scientific, 2002, Ed. Giovanni G. Fazio, page 166.
- [49] M. Centelles, X. Roca-Maza, X. Vinas, and M. Warda, Phys. Rev. C **82** (2010) 054314.
- [50] S. Mizutori, J. Dobaczewski, G. A. Lalazissis, W. Nazarewicz, and P. G. Reinhard, Phys. Rev. C **61** (2000) 044326.
- [51] O. Wieland, and A. Bracco, Progr. Part. Nucl. Phys. **66** (2011) 374; X. Y. Sun *et al.*, Nucl. Phys. **A834** (2010) 502c; A. Ozawa, T. Suzuki, and I. Tanihata, Nucl. Phys. **A693** (2001) 32.
- [52] C. A. Bertulani, Phys. Rev. Lett. **94** (2005) 072701.